metals

MDPI

Article

Magnetostriction of $Ni_2Mn_{1-x}Cr_xGa$ Heusler Alloys

Takuo Sakon [1,*], Naoki Fujimoto [1], Takeshi Kanomata [2] and Yoshiya Adachi [3]

1 Department of Mechanical and System Engineering, Faculty of Science and Technology, Ryukoku University, Otsu 520-2194, Shiga, Japan; t140307@mail.ryukoku.ac.jp
2 Research Institute for Engineering and Technology, Tohoku Gakuin University, Tagajo 985-8537, Miyagi, Japan; kanomata@mail.tohoku-gakuin.ac.jp
3 Graduate School of Science and Engineering, Yamagata University, Yonezawa 992-8510, Yamagata, Japan; adachy@yz.yamagata-u.ac.jp
* Correspondence: sakon@rins.ryukoku.ac.jp; Tel.: +81-77-543-7443

Received: 12 August 2017; Accepted: 28 September 2017; Published: 1 October 2017

Abstract: Among the functionalities of magnetic Heusler alloys, magnetostriction is attracting considerable attention. The alloy Ni_2MnGa has a premartensite phase, which is a precursor state to the martensitic transition. Some researchers have observed magnetostriction in this alloy in the premartensite phase. We performed magnetostriction studies on the premartensite phase of related Cr-substituted $Ni_2Mn_{1-x}Cr_xGa$ alloys and measured the thermal strain, permeability, magnetisation, and magnetostriction of polycrystals. Our thermal expansion measurements show an anomaly that indicates the occurrence of lattice deformation below the premartensitic transition temperature T_P. Our permeability measurements also showed an anomaly at the premartensitic transition. From our magnetisation results, we obtained the magnetic-anisotropy constant K_1. In the martensite phase, we found that the magnetic-anisotropy constant of the x = 0.00 alloy is larger than that of the x = 0.15 alloy. At 0.24 MA/m, we obtained a magnetostriction of −120 ppm for the x = 0.15 alloy. Magnetostriction in the premartensite phase is larger than that in the austenite and martensite phases at low magnetic-field strength, thus indicating that it is related to lattice softening in the premartensite phase. The *e/a* is proportional to the magnetostriction and T_P, which indicates that the electron energy, the magnetostriction, and the T_p are correlative each other.

Keywords: shape-memory alloys; premartensitic transition; thermal expansion; magnetostriction

1. Introduction

1.1. Magnetostriction and Magnetic Field-Induced Strain of Ferroagnetic Shape Memory Alloys

Recently, ferromagnetic shape-memory alloys (FSMAs) have been studied extensively as candidates for highly functional magnetostriction materials for use as actuators, tremblers, and magnetic sensors. Among FSMAs, the alloy Ni_2MnGa is the most well-known [1]. It has a cubic $L2_1$ type Heusler structure (space group $Fm\bar{3}m$) and a ferromagnetic transition that occurs at the Curie temperature T_C = 365 K [2,3]. During cooling from ambient temperature, a martensitic transition occurs at the martensite transition temperature T_M = 200 K. Below T_M, a superstructure state develops as a result of lattice modulation [4,5]. Conventional magnetostriction is the distortion of crystal lattice caused by the rotation of the magnetic moment. FSMAs can induce large strain through martensitic transition or rearrangements of variants induced by external magnetic fields. This is called "twinning magnetostriction", which was discovered by Ullakko and colleagues [1,6]. They discovered 1.5 × 10^3 ppm magnetostriction for a single crystal of Ni-Mn-Ga. This value is comparable to the magnetostriction of 3d/rare-earth intermetallic compounds $TbFe_2$, $DyFe_2$ [7] and $Tb_{0.3}Dy_{0.7}Fe_2$ (terfenol-D) [8]. The reverse transition from martensite phase to parent phase in magnetic fields—which

is called magnetic-field-induced strain (MFIS)—can be observed for FSMAs. The large MFIS was mainly caused by the reorientation of variants and was highly sensitive to the temperature.

The MFIS of a single crystal of $Ni_{52}Mn_{23}Ga_{25}$ exhibited a martensitic transition at room temperature [9]. A large MFIS of −2700 ppm was obtained at 303 K and under atmospheric pressure. A net MFIS of 5400 ppm was induced when a 0.8 MA/m applied field was rotated from the [100] to the [001] directions of the sample. Furthermore, MFISs of 6–10 × 10^3 ppm have been reported in single crystals of Ni_2MnGa near or below room temperature [10]. Some studies have also been conducted on the influence of Fe addition into Ni-Mn-Ga alloys around room temperature [11,12]. A 5.5 × 10^4 ppm MFIS of single-crystal $Ni_{49.9}Mn_{28.3}Ga_{20.1}Fe_{1.7}$ appeared at 293 K [11]. The MFIS of $Ni_{52}Mn_{16}Fe_8Ga_{24}$ single-crystal was 1.15 × 10^4 ppm at 293 K [12]. These MFIS were observed in the martensite phase.

The magnetostriction in polycrystalline $Ni_{50}Mn_{23.1}Ga_{24.6}$ was studied, which shows a martensitic transition at the martensite starting temperature T_{Ms} = 250 K [13]. The number of valence electrons per atom, e/a, for this alloy is 7.57, which is higher than that for Ni_2MnGa (e/a = 7.50). A 540 ppm magnetostriction was observed at T_{Ms}.

Near T_M, lattice softening was observed. Therefore, the physical relation between the magnetostriction and the lattice softening around T_M is interesting. The elastic constants of a $Ni_{0.50}Mn_{0.284}Ga_{0.216}$ single crystal were studied by using the ultrasonic continuous-wave method [14]. They investigated the C_{11}, C_{33}, C_{66}, and C_{44} modes, and found that every mode exhibited abrupt softening around T_M. This lattice softening appears to be affected by the abrupt expansion that occurs just above T_M when cooling from the austenite phase.

1.2. Magnetostriction in Premartensite Phase

The temperature of the martensitic transition is very sensitive to the ratio of constitutive elements for ordered compounds close to stoichiometry, Ni_2MnGa. Between a martensitic transition from a cubic phase (austenite) to a low symmetry phase (martensite), an intermediate phase appears. This intermediate phase is preceded by a so-called "premartensite phase". The premartensitic transition between austenite phase and premartensite phase is weakly first-order and originates from softening of the shear elastic coefficient $C' = (C_{11} - C_{12})/2$ [15–17] corresponding to a minimum on the slowest transversal phonon branch [3,18,19]. Lattice softening is the physical reason for the large variation observed at the martensitic transformation temperature [20]. At the transition, the material exhibits some kind of anomaly in the elastic [16,21], thermal [15], electric [22], and magnetic properties [20,23]. As for $Ni_{2+x}Mn_{1-x}Ga$ polycrystal, the resistivity demonstrates either a peak (x = 0.00−0.04 samples) or a two-step-like behaviour (x = 0.06−0.08 samples) at the premartensitic transition temperature, T_P [22]. The permeability demonstrates a dip at T_P [23]. Singh et al. [24] have suggested that a 3M-like incommensurate premartensite phase exists in Ni_2MnGa.

The feature of the premartensite phase is that magnetostriction occurs. Clear magnetostrictions were observed around T_p in Ni_2MnGa alloys. A minimum was found in both the magnetostriction and the elastic modulus at T_p and at the martensitic transition temperature T_M in single crystalline Ni_2MnGa [17,25]. Matsui et al. [26] investigated magnetostriction in polycrystalline Ni-Mn-Ga alloys and found a magnetostriction of −190 ppm in the premartensite phase—more than three times the amount in the austenite phase. Magnetostriction measurements were performed on polycrystalline Ni_2MnGa [20]. It was found that the saturation magnetostriction was negative, took on moderate values of approximately −100 ppm, and increased greatly in absolute value at both the premartensitic and martensitic transition temperatures, which arise from lattice softening at the transitions. In this study, we performed the measurements of the thermal strain, permeability, magnetisation, and magnetostriction of Cr-substituted $Ni_2Mn_{1-x}Cr_xGa$ alloys.

1.3. Purpose of This Study

We chose $Ni_2Mn_{1-x}Cr_xGa$ because the physical properties of Ni_2MnGa undergo sudden changes with heat treatment. Therefore, we studied the physical properties of doped systems that could predict

high thermal stability. The values of T_C and T_M for the Ni_2MnGa alloys change drastically when they are doped by replacing Mn with a fourth element, such as Fe, Co, Ni, or Cu [27–30]. For example, replacing Mn by Co, Ni, or Cu increases T_M, but the value of T_M for $Ni_2Mn_{1-x}Fe_xGa$ decreases with increasing Fe concentration x. Several authors have shown that the number of e/a is closely related to the value of T_M for Ni-Mn-based FSMAs: a large e/a value indicates a high T_M [31–33]. However, a larger e/a corresponds to a lower T_M for $Ni_2Mn_{1-x}Fe_xGa$ as mentioned above. For $Ni_2Mn_{1-x}Cr_xGa$ alloys, e/a decreases with Cr concentration x (7.50 for x = 0.00 and 7.46 for x = 0.15). Therefore, it would be interesting to know whether the relationship between T_p or magnetostriction and e/a applies to $Ni_2Mn_{1-x}Cr_xGa$. The e/a becomes smaller when Mn ($3d^54s^2$) is replaced by Cr ($3d^54s$). We are interested to investigate a correlation of magnetostriction and e/a which is larger and smaller than 7.50 with a result of the magnetostriction measurements of other Ni-Mn-Ga alloys.

Now we will discuss the physical properties of $Ni_2Mn_{1-x}Cr_xGa$ alloys. As for $x \leq 0.25$, two anomalies were observed on the ρ-T curves for each sample, corresponding to the magnetic and structural phase transitions at the Curie temperature T_C and the martensitic transition temperature T_M [34]. Kinks corresponding to the premartensitic transition at the critical temperature T_P also appeared. A clear variation was observed below the premartensitic transition temperature T_P, thus indicating that lattice deformation occurs below T_P. The martensite-austenite phase transition was investigated for a series of $0 \leq x \leq 0.7$ Heusler alloys by using X-ray diffraction, DC magnetisation, and electrical resistivity measurements [35]. For $x < 0.20$, a ferromagnetic premartensite state appeared below T_P. As the Cr concentration x increased, the martensitic phase transition shifted to higher temperatures, whereas the ferromagnetic transition shifted to lower temperatures. For $x < 0.5$, the martensitic transition occurred in a ferromagnetic state; however, for $x > 0.5$, the transition occurred in a paramagnetic state. Doping with Cr results in a rearrangement of the electronic structure, particularly near the Fermi level. This phenomenon is clearly shown by the resistivity data, where a systematic jump-like anomaly was observed in the vicinity of the martensite–austenite phase transition.

The purpose of this study is to investigate the magnetic properties of $Ni_2Mn_{1-x}Cr_xGa$ alloys more deeply than former studies. From the permeability and magnetization results, the magnetic-anisotropy constants in the three phases (austenite, premartensite, martensite) were obtained. The magnetostriction of the polycrystals of Ni_2MnGa (x = 0.00) and $Ni_2Mn_{0.85}Cr_{0.15}Ga$ (x = 0.15)—both of which have austenite, premartensite, and martensite phases—were performed. We compared them with each other and with $Ni_2Mn_{0.75}Cr_{0.25}Ga$ (x = 0.25), which also has austenite and martensite phases. The relation between the magnetic anisotropy and the magnetostriction was investigated. The relations between the e/a and magnetostriction and T_p were also investigated, and proportional relations were obtained.

2. Materials and Methods

We prepared polycrystalline $Ni_2Mn_{1-x}Cr_xGa$ alloys by the repeated arc-melting of appropriate quantities of the constituent elements—namely, 3N Ni, 4N Mn, 4N Cr and 6N Ga—in an argon atmosphere. The reaction products were sealed in evacuated silica tubes, heated at 1073 K for three days and at 773 K for two more days, and then quenched in water. We employed strain gauges (KFL-02-120-C1-16, size: sensor grid 0.2 mm length × 1.0 mm width, film base 2.5 mm length × 2.2 mm width. Kyowa Dengyo Co. Ltd., Yamagata, Japan) to measure the thermal strain and magnetostriction of bulk samples with sizes of 3.0 mm × 3.0 mm × 4.0 mm. The zero point of the linear thermal strain $\Delta L/L$ was set at 273.15 K, and the rate of temperature change rate was 2 K/min. For the magnetostriction measurements, we applied magnetic fields by using a water-cooled magnet. We employed two gauges, and we applied the magnetic field parallel to (strain $\lambda_{//}$) and, separately, perpendicular to (strain $\lambda_{\perp}$) the gauges. The magnetic-field change rate was 8.8 kA/(ms). We calculated the magnetostriction λ from the equation $\lambda = 2(\lambda_{//} - \lambda_{\perp})/3$ (see [36]). Magnetostriction measurements were also performed during cooling. We performed the permeability measurements in alternating magnetic fields with a frequency of 73 Hz and a maximum field of ±0.8 kA/m (±10 Oe), which we

verified using an magnetometer. We also employed a 3611 filter amp (NF Co. Ltd., Yokohama, Japan) and a 2000/J digital voltmeter (Keithley Co. Ltd, Salem, OR, USA). The measured temperature ranged between 150 K and 400 K. The rate of temperature change was 2 K/min, the same as we used for the linear-strain measurements. We performed the magnetisation measurements by using a pulsed-field magnet with the time constant of 6.3 ms. The absolute value was calibrated against a sample of pure Ni. The bulk samples used in other measurements were also used to compare the results with each other.

3. Results and Discussion

Figure 1 shows the temperature dependence of the linear strain $\Delta L/L$ in the (a) x = 0.00 alloy; (b) x = 0.15 alloy in zero field during cooling and heating. A jump is clearly seen between 195 K and 175 K in x = 0.00 alloy, and between 205 K and 195 K in x = 0.15 alloy, because of the martensitic transition during cooling and the reverse-martensitic transition during heating. In each alloy, approximately 1000 ppm shrinkage was observed during the martensitic transition in the cooling process. Linear strain measurements of single crystalline Ni_2MnGa [1] and polycrystalline $Ni_{49.6}Mn_{27.3}Ga_{23.1}$ [37] were performed. The strain values were practically the same as our result. Those results were less sensitive than our measurement. Therefore, our measurements are of higher resolution. Our result is comparable to the thermal strain observed by Albertini et al. [38] in polycrystalline Ni_2MnGa.

Hysteresis is clearly seen between the martensitic and reverse-martensitic transitions, thus indicating that the martensitic transition is a first-order phase transition. Identical T_P values were obtained for the cooling and heating processes; the difference was at most 0.2 K. Singh et al. [24] suggested from their high-resolution X-ray spectroscopy of single-crystal Ni_2MnGa that a 3M-like structure develops in the premartensite phase. Considering this X-ray spectroscopy result, the linear thermal expansion results of polycrystalline sample in this study indicate that lattice deformation occurred below T_P.

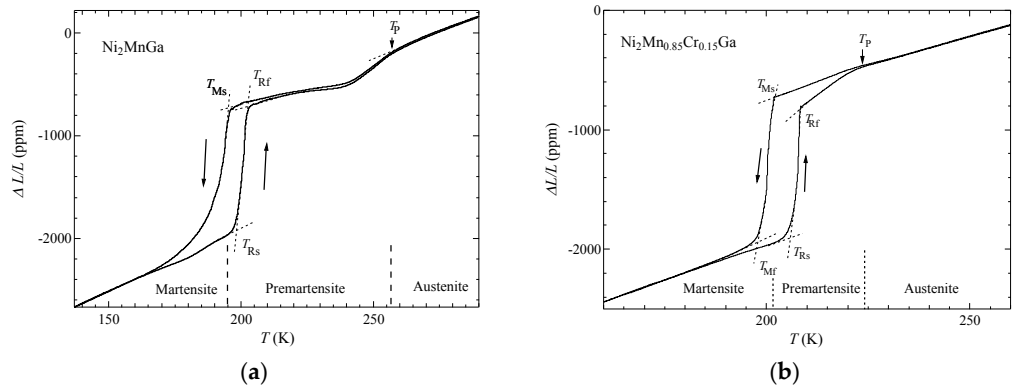

Figure 1. Temperature dependence of the linear strain $\Delta L/L$ in the (**a**) x = 0.00 alloy; and (**b**) x = 0.15 alloy. The quantity T_{Rs} is the temperature where the reverse-martensitic transition starts; T_{Rf} is the temperature where the reverse-martensitic transition ends; T_{Ms} is the temperature where the martensitic transition starts; and T_{Mf} is the temperature where the martensitic transition ends. The dotted lines are intended to guide the eye.

Figure 2 shows the permeability μ of the (a) x = 0.00 alloy; and (b) x = 0.15 alloy during heating and cooling in zero magnetic fields. For x = 0.00, the anomalies or jumps appeared at the martensitic transition at approximately 195 K, the premartensitic transition at approximately 255 K (at which the temperature shows a dip, which was as same as single crystal [23]), and the ferromagnetic transition at approximately T_C = 375 K. When cooling from 400 K through the austenite paramagnetic phase, the value of μ increases at approximately 375 K, thus indicating a ferromagnetic transition in the austenite phase. The μ value dips slightly below 255 K and decreases strongly below 195 K. The permeability curve indicates that the magnetic anisotropy is small in the ferromagnetic

austenite and premartensite phases. By contrast, the value of the permeability decreased drastically at the martensite phase transition. This result indicates that the magnetic anisotropy is large in the martensite phase. Considering that the thermal strain (as shown in Figure 1) decreases steeply with cooling between 260 K and 240 K and that the permeability shows a dip in this temperature range, we conclude that lattice deformation occurred because of the premartensitic transition. As a result, lattice deformation increases magnetic anisotropy.

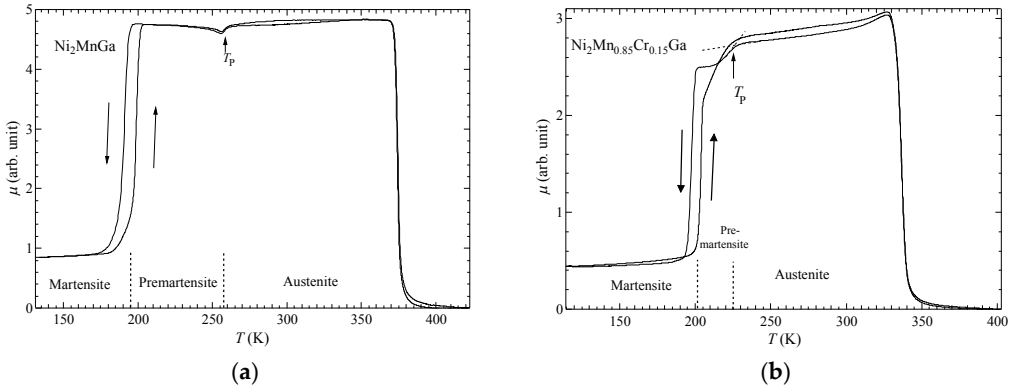

Figure 2. The permeability of the (**a**) $x = 0.00$ alloy; and (**b**) $x = 0.15$ alloy during heating and cooling in zero magnetic fields. The quantity T_P is the premartensitic transition temperature.

As for $x = 0.15$, the anomalies (jumps) are due to the martensitic transition at approximately 200 K, the premartensitic transition at approximately $T_p = 225$ K, and the ferromagnetic transition at approximately $T_C = 340$ K. The μ value dips slightly below 225 K and decreases strongly below 200 K. The magnetisation displays ferromagnetic properties at 5 K, with values of 83 Am^2/kg for the $x = 0.15$ alloy at 4 MA/m [35]. Therefore, the martensite phase is a ferromagnetic phase. The permeability decrease in the ferromagnetic phase below 225 K is believed to be due to magnetic anisotropy. The permeability of $Ni_{50.9}Mn_{24.6}Ga_{24.5}$ exhibited a dip around T_p, whereas $Ni_{48.3}Mn_{24.6}Ga_{24.5}Co_{2.6}$ showed a gradual decrease below T_p. $Ni_{50.9}Mn_{24.6}Ga_{24.5}$ and $Ni_{48.3}Mn_{24.6}Ga_{24.5}Co_{2.6}$ have the same properties at $x = 0.00$ and $x = 0.15$, respectively [39]. The hysteresis (difference in cooling and heating process) of μ of $x = 0.15$ in the premartensite phase is presumed to be due to the difference of the nucleation in the premartensite phase in cooling and heating process. The permeability of No. 3 ($Ni_{51.7}Mn_{24.3}Ga_{24.0}$ polycrystal, $T_{Ms} = 265$ K, $T_{Rf} = 273$ K, $T_p = 285$ K) shows clear hysteresis in the premartensite phase [40]. The difference between T_{Ms} and T_p, $\Delta T = T_p - T_{Ms} = 20$ K. This is smaller than $\Delta T = 63$ K for $x = 0.00$ in this work. As for $x = 0.15$, $\Delta T = 25$ K. Therefore, it is supposed that the hysteresis of the permeability appears when ΔT is small.

When the magnetic anisotropy is small, the magnetic moments are easily directed along the applied alternative magnetic fields in permeability measurements. By contrast, large magnetic anisotropies mean that the magnetic moments are less easily directed along the applied AC magnetic fields. In the ferromagnetic martensite phase (tetragonal symmetry), the magnetic anisotropy is larger than in the austenite phase (cubic symmetry), thus indicating that the permeability is small [41]. Taken together, the permeability decreased below 225 K as shown in Figure 2b and the linear-strain anomaly below T_P shown in Figure 1b imply that lattice deformation and the change of magnetic anisotropy have occurred because of the premartensitic transition. The T_C values for cooling and heating are almost the same, consistent with the linear-strain results. The T_P values found for cooling and heating are also the same. Soto et al. [42] studied Fe-doped NiMnGa ($Ni_{52.5-x}Mn_{23}Ga_{24.5}Fe_x$) alloys, finding that the premartensitic transition temperature was 186 K for the $x = 4.4$ alloy. No significant thermal hysteresis was detected at the premartensitic transition, and no appreciable features were observed in the calorimetric curves at the premartensitic transition. By contrast, our permeability measurements showed a small dip at the premartensitic transition, and the linear

strain and permeability exhibited clear variations for the $x = 0.15$ alloy. Uijttewaal et al. [43] state that the contributions of both magnons and phonons to the free energy of premartensite and austenite only "slightly differ" and that the existence of the premartensitic transition results from a delicate interplay between the vibrational and magnetic excitation mechanisms. We considered that the clear variation in the linear strain indicates lattice deformation and a softening of the lattice. Therefore, changes in the magnetic state are ultimately reflected in the permeability changes.

Figure 3 shows the magnetisation curve for the (a) $x = 0.00$ alloy and (b) $x = 0.15$ alloy measured during cooling process. As for $x = 0.00$, the magnetisation becomes almost saturated around 0.24 MA/m above 220 K, thus indicating that the magnetic anisotropy is small. At 200 K, which is slightly higher than T_{Ms}, the magnetisation increases steeply from 0 MA/m. This value is comparable to the results for the permeability at 200 K because the gradient of the magnetisation is proportional to the permeability. In the martensite phase at 150 K, the magnetisation increases gradually with increasing magnetic-field strength because of large magnetic anisotropy. The properties of magnetisation curves for $x = 0.15$ are almost the same as those for the $x = 0.00$ alloy.

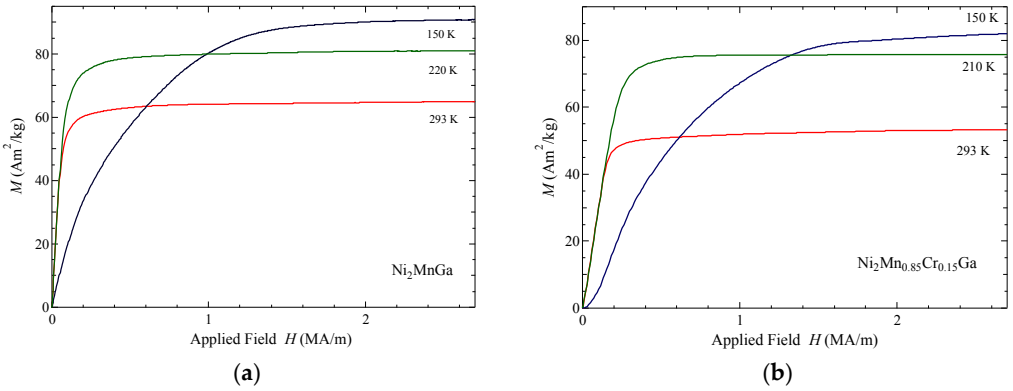

Figure 3. The magnetisation M of the (**a**) $x = 0.00$ alloy; and (**b**) $x = 0.15$ alloy. Blue: martensite phase, Green: premartensite phase, Red: austenite phase.

To determine the amount of magnetic anisotropy, we determined the magnetic-anisotropy field H_{A} from the magnetisation results. This quantity was obtained by the peak of the twice-differentiated magnetisation curve, $d^2M/d\ (\mu_0 H)^2$, by means of the derivation method of H_{A} by the analysis of the magnetization of Ni_2MnGa by Chu et al. [44]. The magnetic-anisotropy constant K_1 is then provided by the equation $K_1 = \mu_0 M_{\mathrm{S}} H_{\mathrm{A}}/2$ [38,44], where M_{S} is the saturation value of the magnetisation. This approach is not the actual way to properly determine the magnetic anisotropy, and might be an approximation. Therefore, error bars are indicated in Figure 4a,b. The resulting values of H_{A} and K_1 are shown in Figure 4a,b, respectively. From the saturated magnetisation M_{s} obtained from the magnetisation curves in Figure 3 and from these values of H_{A}, we found the value of K_1 at 150 K in the martensite phase to be $K_1 = 4.0 \times 10^6$ erg/cm^3 in cgs-emu unit. This value is comparable to other results for K_1 [38,44]. The values of K_1 at 220 K in the premartensite phase and at 293 K in the austenite phase are similarly found to be $K_1 = 0.34 \times 10^6$ erg/cm^3 and $K_1 = 0.30 \times 10^6$ erg/cm^3, respectively, approximately one-tenth of the value at 150 K. Albertini [38] also suggested that the value of K_1 above the martensitic transition temperature is smaller than that in the martensite phase.

As for $x = 0.15$, the H_{A} at 150 K in the martensite phase is smaller than that for the $x = 0.00$ alloy at 150 K. Above T_{Ms}, the H_{A} is considerably smaller than at 150 K in the martensite phase. Conversely, the values of H_{A} in the premartensite and austenite phases are larger than those for the $x = 0.00$ alloy. The resulting value of K_1 at 150 K in the martensite phase is $K_1 = 3.1 \times 10^6$ erg/cm^3, whereas the values at 210 K in the premartensite phase and at 293 K in the austenite phase are $K_1 = 1.0 \times 10^6$ erg/cm^3 and $K_1 = 0.58 \times 10^6$ erg/cm^3, respectively. Similar to the case for the $x = 0.00$ alloy, the permeability exhibits a small dip around T_{p}. By contrast, we found a large decrease below T_{p} for the $x = 0.15$ alloy.

This result indicates that both the magnetic anisotropy and the value of K_1 in the premartensite phase for $x = 0.15$ are larger than those for $x = 0.00$.

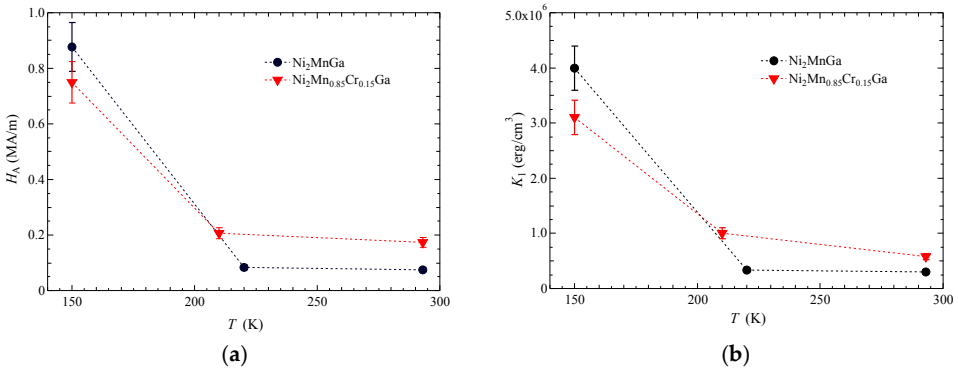

Figure 4. (**a**) The temperature dependence of the magnetic-anisotropy field H_A; (**b**) The temperature dependence of the magnetic-anisotropy energy K_1. The error bars were indicated.

We measured the magnetostriction by using the two-gauge method described in Section 2. Figure 5 shows the magnetostriction for the (a) $x = 0.00$ alloy; and (b) $x = 0.15$ alloy. As for $x = 0.00$, the magnetostriction saturated above 0.08 MA/m in the austenite and premartensite phases. This finding is consistent with the value of the magnetic-anisotropy field $H_A = 0.083$ MA/m at 220 K (premartensite). By contrast, at 162 K in the martensite phase, the magnetostriction increased with increasing field strength, although it showed indications of saturation at 1.27 MA/m. In other words, in order to generate a high driving force for the magnetic domains variants, highly anisotropic and highly saturated magnetisation values are needed [9]. In the austenite and premartensite phases, the magnetic anisotropy was small; therefore, the motive force acts only below 0.083 MA/m. However, in the martensite phase, the anisotropy field and the magnetic-anisotropy constant K_1 were large (as mentioned above, the value of K_1 in the martensite phase was more than 10 times larger than that in the premartensite phase). Therefore, under weak magnetic fields, the variants cannot move because of the high magnetic anisotropy. The motive force then acts until 1.27 MA/m, and large magnetostriction was observed. Regarding $x = 0.15$, a magnetostriction of -120 ppm was observed in the premartensite phase. In the austenite and premartensite phases, the magnetostriction saturated above 0.24 MA/m, which corresponds to the anisotropic field $H_A = 0.21$ MA/m obtained from the magnetisation curves at 210 K. The magnetostriction in the martensite phase (181 K in Figure 5b) saturated at 0.95 MA/m, which is comparable to the value of $H_A = 0.75$ MA/m at 150 K. Considering the permeability shown in Figure 2b and the magnetisation plotted in Figure 3b, we conclude that this result is due to the large magnetic anisotropy in the martensite phase.

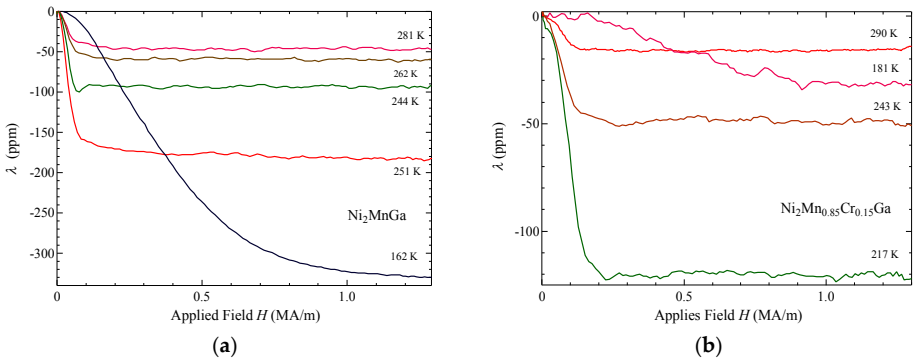

Figure 5. The magnetostriction λ for the (**a**) $x = 0.00$ alloy; and (**b**) $x = 0.15$ alloy, measured during cooling. The horizontal axis shows the applied magnetic field H.

Figure 6 shows the temperature dependence of the magnetostriction values for the (a) x = 0.00 alloy and (b) x = 0.15 alloy. As for x = 0.00, in the austenite phase, the magnetostriction value was approximately −60 ppm at 290 K, and the absolute magnetostriction value increased slightly with cooling. In the premartensite phase, the absolute magnetostriction value increased drastically, reaching a magnetostriction value of −180 ppm at 250 K. The sudden decrease between 260 K and 240 K in Figure 6a corresponds to the temperature range in which the dip in permeability is seen (Figure 2a). Singh et al. [24] suggested that a 3M premartensite phase appears below T_P; therefore, the magnetostriction is correlated with lattice deformation and magnetic anisotropy. Ultrasonic measurements indicate that the shear elastic C' coefficient, $C' = (C_{11} - C_{12})/2$, decreases around T_P [17], indicating that lattice softening occurred around T_P. The magnetostriction at 1.27 MA/m increased drastically around the martensitic transition temperature T_M. At 162 K, we observed a magnetostriction of −330 ppm. This temperature dependence of the magnetostriction has the same shape as the magnetostrain of Ni_2MnGa single crystals measured at 0.4 MA/m [25]. Figure 6a also shows the temperature dependence of the magnetostriction at 0.080 MA/m, as indicated by the triangle symbols. The value of the magnetic-anisotropy field H_A in the austenite and premartensite phases is approximately 0.083 MA/m; we also show the magnetostriction values at 0.080 MA/m near H_A in Figure 6a. A sharp peak can be observed just below the premartensitic transition temperature T_p (which was defined by the thermal strain measurement in Figure 1a). In the martensite phase, the magnetic anisotropy is larger than in the premartensite phase, thus indicating that the variants cannot move in low magnetic fields. As for x = 0.15, the temperature dependence of the saturated magnetostriction values at 0.24 MA/m is equal to the anisotropic field in the austenite and premartensite phases. The full width at half maximum (FWHM) of the peak in the premartensite phase is 20 K. By contrast, the FWHM for the x = 0.00 alloy (Figure 6a) is only 10 K, thus indicating that the anomaly (dip) in the permeability of the x = 0.15 alloy is larger than that of the x = 0.00 alloy.

In the martensite phase, the magnetostriction for the x = 0.15 alloy at 1.27 MA/m and 180 K (−35 ppm) was noticeably smaller than that of the x = 0.00 alloy at 1.27 MA/m and 163 K (−330 ppm); the temperature was approximately 35 K lower than T_{Ms}. This finding suggests that the amount of magnetostriction decreased with increasing Cr concentration. We also measured the magnetostriction for an x = 0.25 alloy, which had a martensitic transition starting temperature T_{Ms} = 214 K.

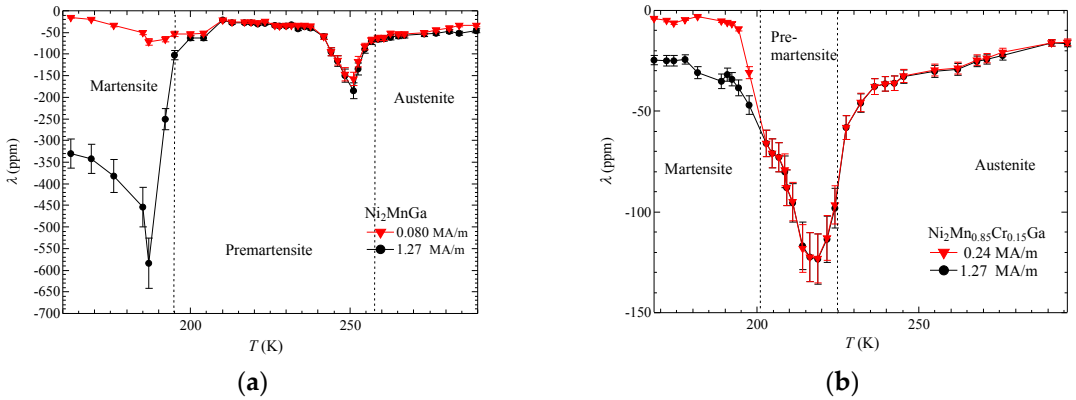

Figure 6. Temperature dependence of the magnetostriction λ for the (**a**) x = 0.00 alloy; and (**b**) x = 0.15 alloy.

Figure 7 shows the temperature dependence of the magnetostriction for the x = 0.25 alloy at 1.27 MA/m, which peaks around T_{Ms}. This property is the same as for the $Ni_{52.3}Mn_{23.1}Ga_{24.6}$ and Ni_2MnGa alloys [13,26]. The magnetostriction of the x = 0.25 alloy at 1.27 MA/m in the martensite phase is between −30 ppm and −35 ppm, which is equal to that of the x = 0.15 alloy. These results confirm that the magnetostriction decreases with increasing Cr concentration. For the x = 0.00 alloy, the magnetic-anisotropy constant (K_1 = 4.0 × 10^6 erg/cm^3) was larger than that for the x = 0.15

alloy (K_1 = 3.1 × 10^6 erg/cm^3). The magnetisation value for the x = 0.00 alloy was also larger than that for x = 0.15. We conclude that larger magnetic anisotropy and larger magnetisation generate larger magnetostriction. However, the change in the amount of magnetostriction is considerably larger than the changes in magnetisation or magnetic anisotropy. Matsui et al. [40] measured the magnetostriction of a Si-doped Ni_2MnGa polycrystal and found that the amount of magnetostriction in the martensite phase was considerably smaller than that of a Ni_2MnGa polycrystal. Conversely, the MFIS for an Fe-doped $Ni_{52}Mn_{16}Fe_8Ga_{24}$ single crystal is 7.5 × 10^3 ppm, which is twice as large as that of a $Ni_{52}Mn_{24}Ga_{24}$ single crystal (3.5 × 10^3 ppm) [12]. They mentioned that Fe substitution for Mn improves the temperature dependence of MFIS.

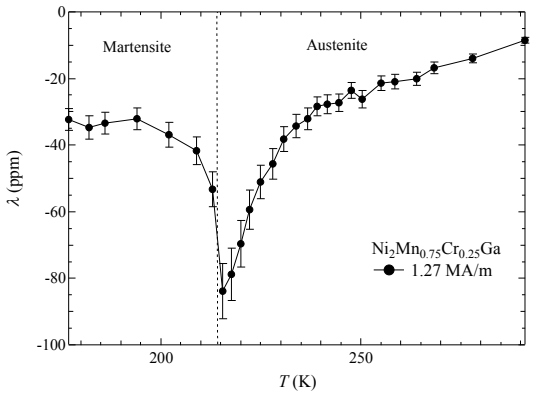

Figure 7. Temperature dependence of the magnetostriction λ for the x = 0.25 alloy.

In order to investigate the relation between valence electron e/a and the magnetostriction value around the premartensitic transition, Figure 8 (a) demonstrates the relationship between e/a and the magnetostriction value around T_P. Figure 8 (b) demonstrates the e/a dependence of the T_P. Table 1 shows the valence electron e/a, the premartensite temperature T_P, and peak value of the magnetostriction around the T_P for each composition. Three Ni-Mn-Ga polycrystals [26,40], two Ni_2MnGa single crystals [17,26], x =0.00, and x = 0.15 were used for this figure. To compare between the polycrystal and single crystal, the magnetostriction λ of the single crystal was calculated as $\lambda \approx 2\lambda_{100}/3$, where λ_{100} is the magnetostriction parallel to the [100] axis. The magnetostriction is almost proportional to the e/a. As shown in Figure 8b, the T_p is also almost proportional to the e/a. It was reported earlier that T_p is proportional to the e/a [45]. From these results, it is considered that the electron energy, the magnetostriction, and the T_p are correlated each other. In doped Ni_2MnGa alloys, the e/a values change; therefore, it is considered that the itinerant electric and magnetic states also vary. As a result, the magneto-structural strain (magnetostriction or MFIS) can be changed.

Table 1. The valence electron e/a, the premartensite temperature T_P, and peak value of the magnetostriction around the T_P for each composition. PC: polycrystal; SC: single crystal.

Composition	*e/a*	T_P (K)	λ (ppm)	References
$Ni_{51.7}Mn_{24.3}Ga_{24.0}$	7.59	285	−550	PC Matsui [26,40]
$Ni_{49.9}Mn_{26.2}Ga_{23.9}$	7.54	259	−360	PC Matsui [26,40]
Ni_2MnGa	7.50	259	−227	SC Seiner [17]
Ni_2MnGa	7.50	258	−180	PC This work
$Ni_{49.2}Mn_{26.5}Ga_{24.3}$	7.50	248	−182	SC Matsui [40]
$Ni_{47.9}Mn_{28.0}Ga_{24.1}$	7.47	225	−180	PC Matsui [26,40]
$Ni_2Mn_{0.85}Cr_{0.15}Ga$	7.46	225	−120	PC This work

Further research is needed both for the kinetic physics and for the itinerant magnetism for Ni_2MnGa-related alloys. The martensitic transformation in stoichiometric Ni_2MnGa alloys is preceded

by a weakly first-order transformation from a high-temperature cubic phase to a near-cubic, modulated, intermediate (premartensite) phase related to the presence of a soft phonon mode [46]. The appearance of this transformation has been proposed as a consequence of magneto-elastic coupling. An inelastic neutron-scattering experiment performed in an external magnetic field also indicated a strong magneto-elastic interaction at the premartensitic transition. We conclude that the large magnetostriction of the x = 0.15 alloy is related to lattice softening in the premartensite phase, similar to that with the x = 0.00 alloy. We expect that magnetostriction can be observed in the premartensite phase because of the softening caused by a perturbing magnetic field. Further studies (acoustic measurements, etc.) are needed to clarify these issues.

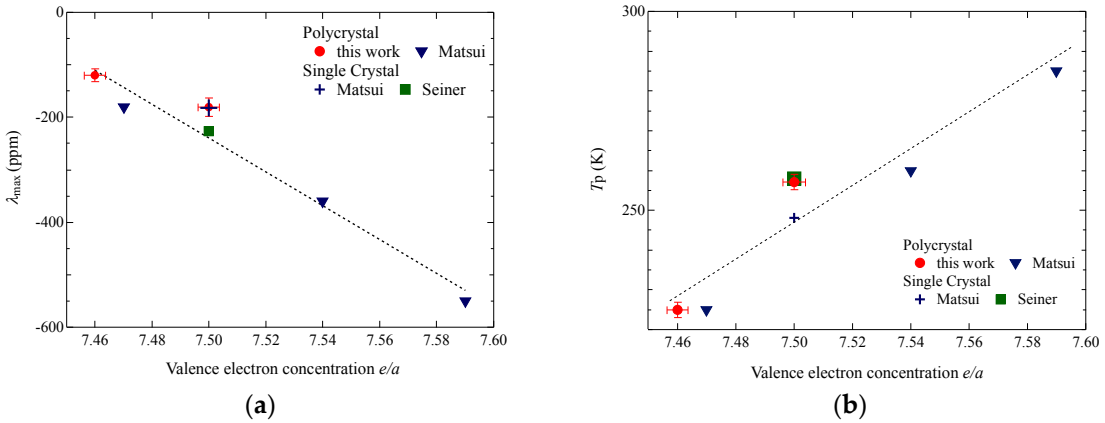

Figure 8. (**a**) The valence electron e/a dependence of peak value of the magnetostriction around the premartensite temperature T_P; (**b**) The valence electron e/a dependence of the T_P. Filled circles: this work. Filled triangles: polycrystal, Matsui et al. [26,40]. Cross: single, Matsui et al. [40]. Filled square: single, Seiner et al. [17]. Dotted lines are fitting lines. The error bars in this work were indicated.

4. Conclusions

We have measured the thermal strain, permeability, magnetisation, and magnetostriction of novel magnetic Heusler $Ni_2Mn_{1-x}Cr_xGa$ polycrystals. The thermal expansion measurements show an anomaly, thus indicating that lattice deformation occurs below the premartensitic transition temperature T_P. The permeability measurements also show an anomaly at the premartensitic transition. From the magnetisation results, we obtained the magnetic-anisotropy constant K_1. In the martensite phase, we found the magnetic-anisotropy constant for the x = 0.00 alloy ($K_1 = 4.0 \times 10^6$ erg/cm^3) to be larger than that for the x = 0.15 alloy ($K_1 = 3.1 \times 10^6$ erg/cm^3). Magnetostriction in the premartensite phase is larger than that in the austenite and martensite phases at low magnetic fields, thus indicating that they are related to lattice softening in the premartensite phase. The magnetostriction and T_P are proportional to the e/a, which indicates that the electron energy, the magnetostriction, and the T_p are correlated each other.

Acknowledgments: The authors would like to express our sincere thanks to Toetsu Shishido and Kazuo Obara in Institute for Materials Research, Tohoku University, and Ryuji Kouta in Facuty of Engineering, Yamagata University for their help on the sample preparation. The authors also thank to Mitsuo Okamoto in Ryukoku University for helping to make the apparatus. This project is partly supported by the Ryukoku Extension Center (REC) at Ryukoku University.

Author Contributions: Yoshiya Adachi prepared the samples; Takuo Sakon and Takeshi Kanomata conceived and designed the experiments; Naoki Fujimoto and Takuo Sakon performed the experiments; Naoki Fujimoto and Takuo Sakon analysed the data; Takuo Sakon and Takeshi Kanomata wrote the paper.

Conflicts of Interest: The authors declare no conflict of interest.

References

1. Ullakko, K.; Huang, J.K.; Kantner, C.; O'Handley, R.C.; Kokorin, V.V. Large magnetic-field-induced strains in Ni_2MnGa single crystals. *Appl. Phys. Lett.* **1996**, *69*, 1966–1968. [CrossRef]
2. Webster, P.J.; Ziebeck, K.R.A.; Town, S.L.; Peak, M.S. Magnetic order and phase transformation in Ni_2MnGa. *Philos. Mag. B* **1984**, *49*, 295–310. [CrossRef]
3. Brown, P.J.; Crangle, J.; Kanomata, T.; Matsumoto, M.; Neumann, K.-U.; Ouladdiaf, B.; Ziebeck, K.R.A. The crystal structure and phase transitions of the magnetic shape memory compound Ni_2MnGa. *J. Phys. Condens. Matter* **2002**, *14*, 10159–10171. [CrossRef]
4. Pons, J.; Santamarta, R.; Chernenko, V.A.; Cesari, E. Long-Period martensitic structures of Ni-Mn-Ga alloys studied by high-resolution transmission electron microscopy. *J. Appl. Phys.* **2005**. [CrossRef]
5. Ranjan, R.; Banik, S.; Barman, S.R.; Kumar, U.; Mukhopadhyay, P.K.; Pandey, D. Powder X-ray diffraction study of the thermoelastic martensite transition in $Ni_2Mn_{1.05}Ga_{0.95}$. *Phys. Rev. B* **2006**. [CrossRef]
6. Ullakko, K.; Huang, J.K.; Kokorin, V.V.; O'Handley, R.C. Magnetically controlled shape memory effect in Ni_2MnGa intermetallics. *Scr. Mater.* **1997**, *36*, 1133–1138. [CrossRef]
7. Clark, A.E.; Belson, H.E. Giant Room-Temperature Magnetostrictions in $TbFe_2$ and $DyFe_2$. *Phys. Rev. B* **1972**, *5*. [CrossRef]
8. Lindgren, E.A.; Haroush, S.; Poret, J.C.; Mazzatesta, A.D.; Rosen, M.; Wun-Fogle, M.; Restorff, J.B.; Clark, A.E.; Lindberg, J.F. Development of Terfenol-D transducer material. *J. Appl. Phys.* **1998**, *83*, 7282–7284. [CrossRef]
9. Yu, C.H.; Wang, W.H.; Chen, J.L.; Wu, G.H.; Yang, F.M.; Tang, N.; Qi, S.R.; Zhan, Z.; Wang, Z.; Zheng, Y.F.; et al. Magnetic-field-induced strains and magnetic properties of Heusler alloy $Ni_{52}Mn_{23}Ga_{25}$. *J. Appl. Phys.* **2000**, *87*, 6292–6294. [CrossRef]
10. Pons, J.; Cesari, E.; Seguí, C.; Masdeu, F.; Santamarta, R. Ferromagnetic shape memory alloys: Alternatives to Ni-Mn-Ga. *Mater. Sci. Eng. A* **2008**, *481–482*, 57–65. [CrossRef]
11. Koho, K.; Söderberg, O.; Lanska, N.; Gea, Y.; Liua, X.; Straka, X.; Vimpari, J.; Heczko, O.; Lindroos, V.K. Effect of the chemical composition to martensitic transformation in Ni-Mn-Ga-Fe alloys. *Mater. Sci. Eng. A* **2004**, *378*, 384–388. [CrossRef]
12. Liu, Z.H.; Zhang, M.; Wang, W.Q.; Wang, W.H.; Chen, J.L.; Wua, G.H.; Meng, F.B.; Liu, H.Y.; Liu, B.D.; Qu, J.P.; et al. Magnetic properties and martensitic transformation in quaternary Heusler alloy of NiMnFeGa. *J. Appl. Phys.* **2002**, *92*, 5006–5010. [CrossRef]
13. Tsuchiya, K.; Ohashi, A.; Ohtoyo, D.; Nakayama, H.; Umemoto, M.; McCormick, P.G. Phase transformation and magnetostriction in Ni-Mn-Ga Ferromagnetic Shape Memory Alloys. *Mater. Trans. JIM* **2000**, *8*, 938–942. [CrossRef]
14. Dai, L.; Cullen, J.; Wuttig, M. Intermartensitic transformation in a NiMnGa alloy. *J. Appl. Phys.* **2004**, *95*, 6957–6959. [CrossRef]
15. Kokorin, V.V.; Chernenko, V.A.; Cesari, E.; Pons, J.; Segui, C. Pre-martensitic state in Ni-Mn-Ga alloys. *J. Phys. Condens. Matter* **1996**, *8*, 6457–6464. [CrossRef]
16. Manosa, L.; Gonzalez-Comas, A.; Obrado, E.; Planes, A.; Chernenko, V.A.; Kokorin, V.V.; Cesari, E. Anomalies related to the TA_2-phonon-mode condensation in the Heusler Ni_2MnGa alloy. *Phys. Rev. B* **1997**, *55*, 11068–11071. [CrossRef]
17. Seiner, H.; Kopeck´y, V.; Landa, M.; Heczko, O. Elasticity and magnetism of Ni_2MnGa premartensitic tweed. *Phys. Status Solidi B* **2014**, *251*, 2097–2103. [CrossRef]
18. Zheludev, A.; Shapiro, S.M.; Wochner, P.; Schwartz, A.; Wall, M.; Tanner, L.E. Phonon anomaly, central peak, and microstructures in Ni_2MnGa. *Phys. Rev. B* **1995**, *51*, 11310–11314. [CrossRef]
19. Stuhr, U.; Vorderwisch, P.; Kokorin, V.V.; Lindgard, P.-A. Premartensitic phenomena in the ferro- and paramagnetic phases of Ni_2MnGa. *Phys. Rev. B* **1997**, *56*, 14360–14365. [CrossRef]
20. Barandiarán, J.M.; Chernenko, V.A.; Gutiérrez, J.; Orúe, I.; Lázpita, P. Magnetostriction in the vicinity of structural transitions in Ni_2MnGa. *Appl. Phys. Lett.* **2012**. [CrossRef]
21. Heczko, O.; Landa, M.; Seiner, H. Anomalous lattice softening of Ni_2MnGa austenite due to magnetoelastic coupling. *J. Appl. Phys.* **2012**. [CrossRef]
22. Khovailo, V.V.; Takagi, T.; Bozhko, A.D.; Matsumoto, M.; Tani, J.; Shavrov, V.G. Premartensitic Transition in $Ni_{2+x}Mn_{1-x}Ga$ Heusler Alloys. *J. Phys. Condens. Matter* **2001**, *13*, 9655–9662. [CrossRef]

23. Chernenko, V.A.; Besseghini, S.; Kanomata, T.; Yoshida, H.; Kakeshita, T. Effect of high hydrostatic pressure on premartensitic transition in Ni_2MnGa. *Scr. Mater.* **2006**, *55*, 303–306. [CrossRef]
24. Singh, S.; Bednarcik, J.; Barman, S.R.; Felsher, S.R.; Pandey, D. Premartensite to martensite transition and its implications for the origin of modulation in Ni_2MnGa ferromagnetic shape-memory alloy. *Phys. Rev. B* **2015**. [CrossRef]
25. Chernenko, V.A.; L'vov, V.A. Magnetoelastic nature of ferromagnetic shape memory effect. *Mater. Sci. Forum* **2008**, *583*, 1–20. [CrossRef]
26. Matsui, M.; Nakakura, T.; Murakami, D.; Asano, H. Super magnetostriction with mesophase transition of Ni_2MnGa. *Toyota Sci. Rep.* **2010**, *63*, 27–36.
27. Kikuchi, D.; Kanomata, T.; Yamaguchi, Y.; Nishimura, H.; Koyama, K.; Watanabe, K. Magnetic properties of ferromagnetic shape memory alloys $Ni_2Mn_{1-x}Fe_xGa$. *J. Alloys Compd.* **2004**, *383*, 184–188. [CrossRef]
28. Khan, M.; Dubenko, I.; Stadler, S.; Ali, N. The Structural and Magnetic Properties of $Ni_2Mn_{1-x}M_xGa$ (M = Co, Cu). *J. Appl. Phys.* **2005**, *97*. [CrossRef]
29. Khovaylo, V.V.; Buchelnikov, V.D.; Kainuma, R.; Koledov, V.V.; Ohtsuka, M.; Shavrov, V.G.; Takagi, T.; Taskaev, S.V.; Vasiliev, A.N. Phase transitions in $Ni_{2+x}Mn_{1-x}Ga$ with a high Ni excess. *Phys. Rev. B* **2005**, *72*. [CrossRef]
30. Kataoka, M.; Endo, K.; Kudo, N.; Kanomata, T.; Nishihara, H.; Shishido, T.; Umetsu, R.Y.; Nagasako, M.; Kainuma, R. Martensitic transition, ferromagnetic transition, and their interplay in the shape memory alloys $Ni_2Mn_{1-x}Cu_xGa$. *Phys. Rev. B* **2010**. [CrossRef]
31. Chernenko, V.A. Compositional Ionsability of β-phase in Ni-Mn-Ga Alloys. *Scr. Mater.* **1999**, *40*, 523–527. [CrossRef]
32. Khovailo, V.V.; Abe, T.; Koledov, V.V.; Matsumoto, M.; Nakamura, H.; Note, R.; Ohtsuka, M.; Shavrov, V.G.; Takagi, T. Influence of Fe and Co on Phase Transitions in Ni-Mn-Ga Alloys. *Mater. Trans.* **2003**, *44*, 2509–2512. [CrossRef]
33. Jin, X.; Marinori, M.; Bono, D.; Allen, S.M.; O'Handley, R.C.; Hsu, T.Y. Empirical mapping of Ni-Mn-Ga properties with composition and valence electron concentration. *J. Appl. Phys.* **2002**, *91*, 8222–8224. [CrossRef]
34. Adachi, Y.; Kouta, R.; Fujii, M.; Kanomata, T.; Umetsu, R.Y.; Kainuma, R. Magnetic Phase Diagram of Heusler alloy system $Ni_2Mn_{1-x}Cr_xGa$. *Phys. Procedia* **2015**, *75*, 1187–1191. [CrossRef]
35. Khan, M.; Brock, J.; Sugerman, I. Anomalous transport properties of $Ni_2Mn_{1-x}Cr_xGa$ Heusler alloys at the martensite-austenite phase transition. *Phys. Rev. B* **2016**. [CrossRef]
36. Mori, K.; Harthway, K.; Clark, A.E. Magnetostriction in polycrystal $Pr_2(Co_{1-x}Fe_x)_{17}$ compounds and their easy directions of magnetization. *J. Appl. Phys.* **1982**, *53*, 8110–8112. [CrossRef]
37. Aksoy, S.; Krenke, T.; Acet, M.; Wassermann, E.F.; Moya, X.; Mañosa, L.; Planes, A. Magnetization easy axis in martensitic Heusler alloys estimated by strain measurements under magnetic field. *Appl. Phys. Lett.* **2007**. [CrossRef]
38. Albertini, F.; Morellon, L.; Algarabel, P.A.; Ibara, M.R.; Pareti, L.; Arnold, Z.; Calestani, G. Magnetoelastic effects and magnetic anisotropy in Ni_2MnGa polycrystals. *J. Appl. Phys.* **2001**. [CrossRef]
39. Soto-Parra, D.E.; Moya, X.; Mañosa, L.; Planes, A.; Flores-Zúñiga, H.; Alvarado-Hernández, F.; Ochoa-Gamboa, R.A.; Matutes-Aquino, J.A.; Ríos-Jara, D. Fe and Co selective substitution in Ni_2MnGa: Effect of magnetism on relative phase stability. *Philos. Mag.* **2010**, *90*, 2771–2792. [CrossRef]
40. Matsui, M.; Nakamura, T.; Murakami, D.; Yoshimura, S.; Asano, H. Effect of Super Magnetostriction on Magnetic Anisotropy of Ni_2MnGa. *Toyota Sci. Rep.* **2011**, *64*, 1–11.
41. Kikuchi, D.; Kanomata, T.; Yamaguchi, Y.; Nishihara, H. Magnetic properties of ferromagnetic shape memory alloys $Ni_{50+x}Mn_{12.5}Fe_{12.5}Ga_{25-x}$. *J. Alloys Compd.* **2006**, *426*, 223–227. [CrossRef]
42. Soto, D.; Alvarado Hernández, F.; Flores-Zúñiga, H.; Moya, X.; Mañosa, L.; Planes, A.; Aksoy, S.; Acet, M.; Krenke, T. Phase diagram of Fe-doped Ni-Mn-Ga ferromagneic shape-memory alloys. *Phys. Rev. B* **2008**. [CrossRef]
43. Uijttewaal, M.A.; Hickel, T.; Neugebauer, J.; Gruner, M.E.; Entel, P. Understanding the Phase Transitions of the Ni_2MnGa Magnetic Shape Memory System from First Principles. *Phys. Rev. Lett.* **2009**. [CrossRef] [PubMed]
44. Chu, S.-Y.; Cramb, A.; De Graef, M.; Laughlin, D.; McHenry, M.E. The effect of field cooling and field orientation on the martensitic phase transformation in a single crystal. *J. Appl. Phys.* **2000**, *87*, 5777–5779. [CrossRef]

45. Wu, S.K.; Yang, S.T. Effect of composition on transformation temperatures of Ni-Mn-Ga shape memory alloys. *Mater. Lett.* **2003**, *57*, 4291–4296. [CrossRef]
46. Recarte, V.; Perez-Landazabal, J.I.; Sanchez-Alarcos, V.; Cesari, E.; Jimenez-Ruiz, M.; Schmalzl, K.; Chernenko, V.A. Direct evidence of the magnetoelastic interaction in Ni_2MnGa magnetic shape memory system. *Appl. Phys. Lett.* **2013**. [CrossRef]